

AN APPROACH OF WEB STIFFENER CALCULATION IN THIN-WALLED COLUMNS

Mantas STULPINAS , Alfonsas DANIŪNAS 

*Department of Steel and Composite Structures, Faculty of Civil Engineering,
Vilnius Gediminas Technical University, Vilnius, Lithuania*

Article History:

- received 14 March 2024
- accepted 19 June 2024

Abstract. This article presents an analytical approach for calculating web stiffeners in thin-walled columns. A novel method is introduced, which treats each bending point in the cross-section web as a separate stiffener. The advantages of this calculation method are discussed, highlighting its increased versatility in designing cross-section geometry. The load-bearing strength of axially compressed thin-walled closed cross-section columns, calculated using this method, is compared to analytical calculations based on the Eurocode 3-1-3 methodology and to the finite element method analysis. Calculation results of columns with cross-sections including shallow web stiffeners were up to 9.22% less conservative when compared to the Eurocode 3-1-3 methodology. The results demonstrate great compliance of the proposed method for column cross-sections with deep stiffeners. Finite element method (FEM) analysis was performed to verify the calculated load bearing strengths of the columns according to both calculation methodologies. FEM analysis confirmed the reliance of the calculated results and showed, that the load bearing strengths calculated using the newly presented methodology were ranging from 88.77% to 97.86% of load bearing strength calculated using finite element method. These results proved, that the proposed method provides an accurate load bearing strength of thin-walled columns with web stiffeners.

Keywords: cold-formed structures, Eurocode, Finite element method, slender members, local buckling, distortional buckling, flexural buckling.

 Corresponding author. E-mail: mantas.stulpinas@vilniustech.lt

1. Introduction

Recent research in steel structures covers various critical topics significant for advancing the field. These include investigations into structural stability (Wen et al., 2024), design and analysis methods (Cheng et al., 2024), connection design (Abdoh, 2024), seismic performance (Mokhtari & Imanpour, 2024), fire performance (Habashneh et al., 2024), life cycle assessment (Seyedabadi et al., 2024), and optimization strategies (Laghi et al., 2024). Steel structures, best known for its high strength-to-weight ratio and durability, remains a frequent material in diverse structural applications, ranging from towering skyscrapers (Zhou et al., 2023) to complicated bridge designs. Engineers, guided by a methodical approach, continually seek to optimize structural solutions, aiming to maximize performance while minimizing material usage and environmental impact (Truong & Chou, 2023). Cold-formed structures, with their simple production techniques and efficient material utilization, often emerge as prime candidates for achieving these sustainability goals in steel structures. However, analysing these structures, particularly those subjected to

compression, presents higher analysis complexity due to the thin-walled configuration of their cross-sections.

Thin-walled columns are widely used in various structural applications due to their lightweight and economic advantages. However, their high slenderness poses challenges in terms of stability and load-bearing capacity. The design of thin-walled column cross-sections requires careful consideration of buckling modes, particularly local and distortional buckling. To enhance their performance, the incorporation of stiffeners in the cross-section has been a subject of extensive research. Research has been done both in design methods of the thin-walled members using finite element methods (FEM) (Zhang & Young, 2018a) or design codes (Alabi-Bello et al., 2021; Weixin et al., 2015) and research in analysis of the connections (Ye et al., 2022; Mojtabaei et al., 2021; Bučmys et al., 2018). Gurupatham et al. (2022) specifically analysed the influence of intermediate stiffeners in thin-walled built-up columns. Thin-walled steel structures, mainly composed of cold-formed members, have traditionally found utility in applications

where substantial load-bearing capacity is not required. These applications often include secondary beams, rack structures (Natali & Morelli, 2022), or lightweight partition walls (Liu et al., 2023). However, advancements in the analysis of cold-formed structures over recent decades have eased their transition into primary building structures (Schafer, 2011; Zhang & Rasmussen, 2014; Rinchen & Rasmussen, 2020). Cold-formed members are easy to transport, stack and assemble as well as being sustainable due to their recyclability and effective use of material (Meza et al., 2020).

In this paper, cross-sections that are suitable for production and utilization in building structures are analysed. Specifically, the investigation concerns closed cross-sections presumed to form through the junction of two distinct open cross-section profiles into a continuous closed configuration. Closed cross-section thin-walled columns are commonly employed in construction due to their superior effectiveness compared to open cross-section thin-walled columns, primarily attributed to the increased torsional buckling stability offered by closed cross-sections. The most practical approach for manufacturing closed thin-walled cold-formed steel members involves connecting two or more profiles using connectors like self-drilling screws. Extensive analysis of built-up thin-walled columns has been conducted in both experimental (Sang et al., 2022; Li & Young, 2023) and numerical studies (Meza & Becque, 2023; Dar et al., 2022). Drawing from the insights acquired by these researchers, this study focuses on the examination of built-up column cross-sections, wherein two "sigma" profiles are interconnected at their flanges, as this method of assembly is relatively straightforward. Cross-section columns of this nature offer enhanced integration into building structures due to the flatness of their flanges and web surfaces, simplifying assembly with other structural elements.

Previous investigations have already examined the overlapping parts in similar configurations. Zhang and Young (2018b) conducted an analysis of two "sigma" profiles connected at the flanges and concluded that considering the overlapping part of the cross-section thickness as equal to the single profile thickness provides reliable and conservative results. Similarly, Kherbouche and Megnounif (2019) examined a comparable cross-section and concluded that such axially compressed column cross-sections can be effectively calculated as a single continuous cross-section. The insights derived from their study were integrated into the analysis of closed cross-section columns presented in this paper.

Another research object for thin-walled structures is longitudinal stiffeners in members. Previous studies have extensively investigated main types of stiffeners used in thin-walled members, including edge stiffeners (Kotenko, 2007; Li & Young, 2024), intermediate stiffeners located within the cross-section's web (Ananthi et al., 2021; Chen et al., 2010; Gurupatham et al., 2022), and those positioned within the flange (Dong & Wen, 2015). While edge stiffen-

ers are restricted to open cross-sections, the effectiveness of intermediate web stiffeners in enhancing the load-carrying capacity of members often surpasses that of intermediate flange stiffeners.

Consequently, this paper focuses on the analysis of intermediate web stiffeners in thin-walled column closed cross-sections. The investigation primarily focuses on their performance concerning distortional buckling resistance and reinforcement of buckling resistance in thin-walled columns. Although finite element method analysis has been employed for columns with intermediate stiffeners, comparing these results with those derived from the Direct Strength Method (DSM) analysis, there is a lack of analytical calculation analysis conforming to the Eurocode 3 design codes for such configurations. This paper proposes a novel design approach for stiffeners in thin-walled columns, drawing upon calculation procedures outlined in the Eurocode 3-1-3 (European Committee for Standardization [CEN], 2006a). It aims to address certain limitations inherent in the code calculation procedures for thin-walled member cross-sections, thereby offering potential enhancements in design practices for such structures. Intermediate stiffeners in thin-walled columns are the main objects in this article. By enhancing our understanding of the web stiffener effects in thin-walled column design, this research aims to contribute to the development of more efficient and accurate structural solutions as well as to expand the analytical calculation limits given in the Eurocode design codes for the thin-walled members with intermediate web stiffeners. The findings of this study have the potential to describe the design process, improve structural performance, and ultimately advance the field of thin-walled column engineering.

2. Eurocode approach for stiffener analysis

Thin-walled cross-section parts exhibit high slenderness, making them vulnerable to buckling. To address this, an effective width algorithm was introduced in Eurocode 3-1-5 (CEN, 2006b), which provides calculation procedures for local buckling of plate elements without longitudinal stiffeners. In these procedures, the cross-section plate parts are idealized, wherein the central portion of the plate is considered ineffective and unable to withstand compressive stresses due to its vulnerability to buckling. However, it is recognized that the corner parts of the plate remain unaffected by local buckling and are considered effective in carrying compressive stresses. To enhance the stability of the cross-section plate element, longitudinal stiffeners are employed. To reinforce compressed thin-walled plate elements, one approach is to add subpanels perpendicular to the plate. Another method involves employing stiffeners. Eurocode 3, Part 1-5 (CEN, 2006b), offers calculation procedures for analysing plate element reinforcement with perpendicular subpanels, while Part 1-3 (CEN, 2006a), addresses procedures for evaluating the distortional buckling of stiffeners in compressed thin-walled member cross-

sections. The latter procedures classify stiffeners into two types: plane elements with edge stiffeners and plane elements with intermediate stiffeners. Although the types differ in their configuration, the calculation basis for both remains similar. The procedure treats the stiffeners to be supported by spring supports. It consists of several steps, beginning with the determination of the initial effective width of the stiffener, assuming it ensures full restraint. The next step involves calculating the reduction factor based on the elastic critical stress of the effective area of the stiffener. Iteratively, the first and second steps can be repeated, adjusting the reduction factor until convergence is achieved with the reduction factor from the previous iteration. Once these steps are completed, the thickness of the stiffener is reduced by the determined reduction factor.

The calculation procedure outlined in Eurocode is applicable to intermediate stiffeners that are formed by grooves or bends. The effective width of each plane element of the stiffener should be calculated independently, treating it as a plane element without stiffeners for assessing local buckling capacity. The cross-sectional area of the stiffener is determined by considering the combination of the plane element of the stiffener and the adjacent effective plane element parts. The geometric representation of the intermediate stiffener according to Eurocode 3-1-3 (CEN, 2006a) is provided in Figure 1. This approach enables a comprehensive analysis of the intermediate stiffeners' contribution to the overall performance of thin-walled columns, allowing for more accurate and efficient design considerations.

The cross-section area of the stiffener is calculated:

$$A_s = t(b_{1,e2} + b_{2,e1} + b_s), \quad (1)$$

where t is the thickness of the cross-section, $b_{1,e2}$ and $b_{2,e1}$ are the effective width of the plane parts of the adjacent plates.

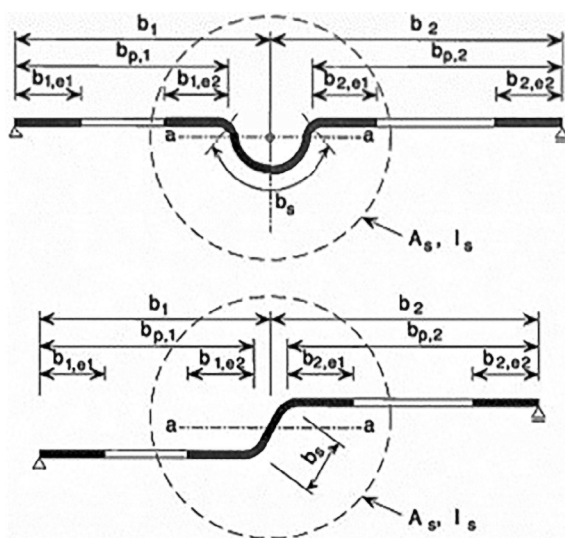


Figure 1. The cross-section area of the intermediate stiffener according to the Eurocode 3-1-3 (CEN, 2006a)

However, the analysis of stiffeners according to the Eurocode is typically restricted to those with low slenderness ratios. Yet, deeper stiffeners with a higher slenderness ratio can offer significant effectiveness, particularly in members characterized by a greater cross-section height. This case often arises in beams and columns subject to bending moments, where increased cross-section height is essential for higher bending stiffness.

Recent findings have indicated that in certain instances, thin-walled columns subjected to axial compression achieve optimal performance with stiffeners of high slenderness (Stulpinas & Daniūnas, 2024). Therefore, this paper proposes an alternative calculation approach for web stiffeners in thin-walled columns, based on the approach given in the Eurocode 3-1-3 (CEN, 2006a), which expands the analytical calculation limits to include stiffeners of higher slenderness. Grounded in the Eurocode methodology, this approach aims to assess stiffener effectiveness and its contribution to the overall load-bearing strength of the column.

3. Proposed stiffener analysis method

This paper introduces a novel concept of employing thin-walled intermediate web stiffeners within column cross-sections. The proposed calculation methodology bears resemblance to the algorithm given in Eurocode 3-1-3 (CEN, 2006a). To explain this approach, comparative analysis between the proposed method and the Eurocode algorithm is presented, highlighting their similarities and differences. The calculation methodology given in Eurocode is tailored for plates featuring one or two stiffeners and is circumscribed by the stiffener's geometry, where the stiffener-part plate remains unaffected by local buckling. In such instances, the width-to-thickness ratio of the stiffener part plate is constrained, particularly for S355 steel grade columns, where this ratio must not exceed 30.

Conventionally, in thin-walled cross-sections with stiffeners, the stiffener's cross-section consists of two bends and a plate part sandwiched between the bends, alongside effective plate parts adjacent to the bends. This stiffener cross-section can be simplified into a triangular groove shape, where the stiffener's cross-sectional area combines with the effective plate parts of adjacent web plates, as depicted in Figure 2a. With the newly proposed design approach it is suggested to treat each bend of the web as an independent stiffener, as illustrated in Figure 2b. Consequently, one stiffener is subdivided into three separate stiffeners, each possessing independent cross-sectional areas and slenderness. This method aims to broaden the design flexibility of stiffener cross-sections, accommodating ineffective cross-section parts between the stiffener bends, as exemplified in Figure 2c. The amount of web bends, as well as separate stiffeners, can be increased, as it is given in Figure 2d.

The following text contains procedures of the proposed thin-walled column web stiffener calculation meth-

od. These procedures are given for representative columns with three and four web bends. These bends are analysed as separate stiffeners. To analyse these stiffeners, effective widths of the plate parts between the web bends are calculated according to the procedures given in the design codes.

The stiffener's cross-sectional area is considered to consist of a bend point and two adjacent effective plate widths. Although the calculation algorithm remains similar to that described in Eurocode 3-1-3 (CEN, 2006a), the stiffener's area is computed differently. The cross-section area of the stiffener for the proposed method is calculated:

$$A_{s,i} = t(b_{i,e2} + b_{i+1,e1}), \quad (2)$$

where t is the thickness of the column cross-section, $b_{i,e2}$ and $b_{i+1,e1}$ are the effective plate widths of the plate parts next to the stiffener bend, i is the number of a stiffener. Figures 2b and 2c depict the cross-sectional areas of the stiffeners where the web consists of three web stiffeners, while Figure 2d illustrates the cross-sectional areas of the stiffeners with four web stiffeners, each accompanied by respective adjacent effective plate widths.

Subsequent to the determination of cross-sectional areas, it becomes necessary to compute the second moment of the cross-section and the associated spring stiffness for each individual stiffener. These calculations are required to determine the critical buckling stress of the stiffeners, which is calculated for each stiffener separately. The critical buckling stress of the stiffeners is based on the expression given in the Eurocode and is calculated as follows:

$$\sigma_{cr,s,i} = \frac{2\sqrt{K_i EI_{s,i}}}{A_{s,i}}, \quad (3)$$

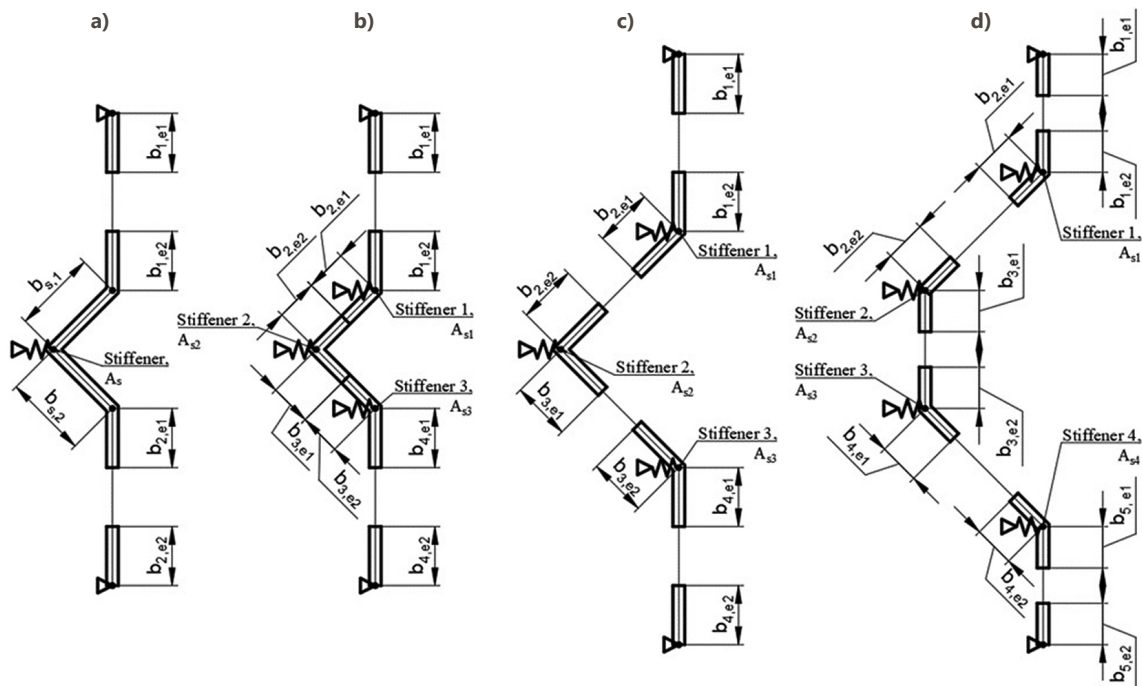


Figure 2. The cross-section area of the intermediate stiffener: a – Eurocode approach; b – proposed approach for a reduced slenderness stiffener; c – proposed approach for a high slenderness stiffener; d – web cross-section with four stiffeners according to the proposed method

where K_i is the spring stiffness of the i -th stiffener ($i = 1, 2, 3, 4$), E is the elasticity modulus, $I_{s,i}$ is the second moment of cross-section area of the i -th stiffener according to the relevant axis, $A_{s,i}$ is the cross-section area of the i -th stiffener.

Following the determination of the critical buckling stress for each stiffener, the relative slenderness of these stiffeners is calculated as follows:

$$\bar{\lambda}_{d,i} = \sqrt{f_{yb} / \sigma_{cr,s,i}}, \quad (4)$$

where f_{yb} is the basic yield strength.

In assessing a stiffener's susceptibility to distortional buckling, essential consideration is the incorporation of a reduction factor applied to the stiffener's cross-sectional area during the computation of its buckling strength. This reduction factor is dependent upon the relative slenderness of the stiffener. Notably, stiffeners characterized by higher relative slenderness ratios undergo a greater reduction in their cross-sectional area, reflecting their increased susceptibility to distortional buckling. The reduction factor for the distortional buckling resistance of each stiffener is calculated:

$$\chi_{d,i} = 1 \quad \text{if } \bar{\lambda}_{d,i} \leq 0.65; \quad (5)$$

$$\chi_{d,i} = 1.47 - 0.723\bar{\lambda}_{d,i} \quad \text{if } 0.65 < \bar{\lambda}_{d,i} < 1.38; \quad (6)$$

$$\chi_{d,i} = \frac{0.66}{\bar{\lambda}_{d,i}} \quad \text{if } \bar{\lambda}_{d,i} \geq 1.38. \quad (7)$$

The reduced effective area of each i -th stiffener when distortional buckling is considered:

$$A_{s,red,i} = \chi_{d,i} A_{s,i} \frac{f_{yb} / \gamma_{M0}}{\sigma_{com,Ed}}, \quad (8)$$

where γ_{M0} is the partial safety factor for the material, $\sigma_{com,Ed}$ is the compressive stress at the centerline of the stiffener calculated on the basis of the effective cross-section.

Concluding the analytical process, the determination of the thickness of each stiffener's cross-section is required. This calculation encompasses the evaluation of the effective plate sections adjoining the bending point of the stiffener, providing an effective stiffener cross-section geometry. The reduced stiffener thickness is calculated:

$$t_{red,i} = \chi_{d,i} t, \quad (9)$$

where t is the thickness of the stiffener.

Following calculations comply to established design codes, integrating the determined effective stiffener cross-sectional areas into the calculations related to the effective column cross-sectional area.

The adoption of the calculation algorithm proposed in this article increases the complexity of stiffener analysis compared to the original methodology given in Eurocode 3-1-3 (CEN, 2006a). However, such calculation assumptions provide a greater flexibility in cross-section geometry design, allowing wider plate elements with potential ineffective areas between bends. Figure 3 illustrates the geometric representations of stiffeners for some cross-section types employing the proposed method. Figure 3a illustrates the full cross-section of columns, while Figure 3b shows the effective area of column cross-sections when calculating according to the design codes for one stiffener and when calculating according to the proposed method for three and four intermediate web stiffeners.

Analogous restrictions regarding cross-section geometry, as given in Eurocode 3-1-3 (CEN, 2006a) and Eurocode 3-1-5 (CEN, 2006b), are relevant when employing the methodology described in this article to calculate column

strength: the width-to-thickness ratio of plate parts of the cross-section must not exceed 500 and the core thickness of the steel plates should range between 0.45 mm and 15 mm. The efficiency of this calculation methodology has been explored through the examination of the columns analysed within the scope of this paper. However, it is necessary to extend this investigation to encompass additional cross-sectional configurations. Such an effort will serve to validate the predictive accuracy of this method concerning load-bearing resistance across diverse typologies of thin-walled columns.

4. Verification of the proposed calculation algorithm

In order to assess the accuracy of the calculated load-bearing strength of axially compressed columns, comparative analytical calculations were conducted. Column cross-section with three different intermediate web stiffener variants was analysed. Width of the cross-section was $b = 60$ mm and height was $h = 150$ mm. Three types of the cross-section were analysed, each including a unique intermediate web stiffener variant. These cross-section variants were named Type A, Type B and Type C and are given in Figure 4. Type A cross-section was engineered with a web height to stiffener depth ratio of $h/15$ (10 mm deep web stiffeners), while Type B cross-section had a ratio of $h/6$ (25 mm deep web stiffeners). Load-bearing strength of the columns was computed using both the method given in Eurocode 3-1-3 (CEN, 2006a) and the approach proposed in this article. Column heights ranging from 3 meters to 5 meters were selected, aligning with common civil engineering standards. Various width-to-thickness ratios of the stiffeners were examined. For Type A cross-sections, these ratios were 30, 20, and 10, corresponding to thicknesses of 0.471 mm, 0.707 mm, and 1.414 mm, respectively. Accordingly, non-dimensional slenderness was equal to 0.650, 0.433 and 0.216. Due to the restriction imposed by the thin-walled cross-section's thickness limit of 0.45 mm, higher ratios for Type A cross-sections could not be analysed. Conversely, Type B cross-sections were subjected to a wider range of width-to-thickness ratios, spanning 50, 40, 30, 20, and 10, corresponding to thicknesses of 0.707 mm, 0.884 mm, 1.179 mm, 1.768 mm and 3.536 mm.

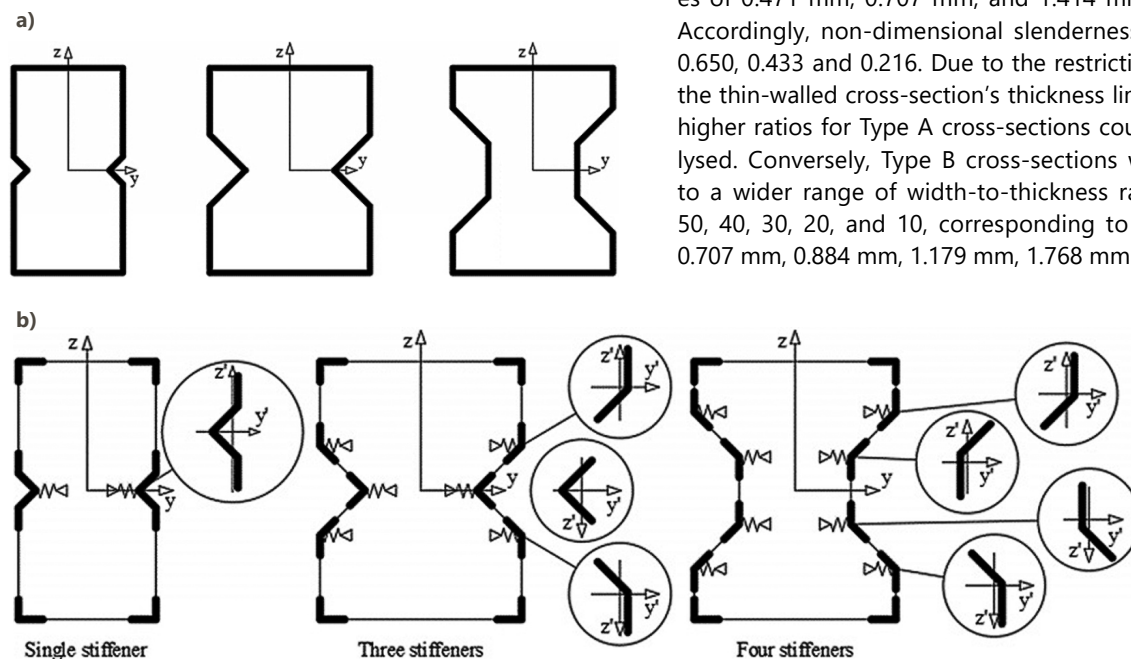


Figure 3. The intermediate web stiffeners of a cross-section: a – full cross-sections; b – models with effective cross-section areas

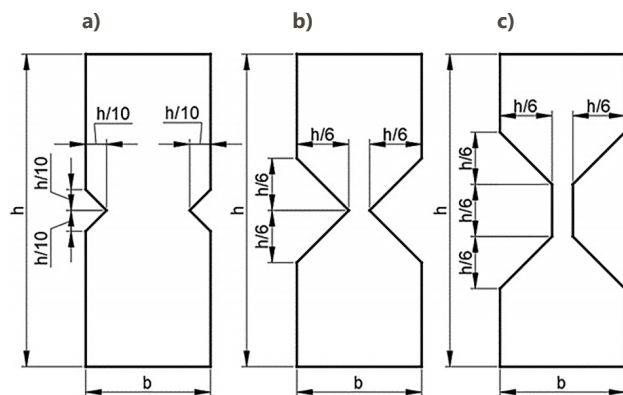


Figure 4. The analysed thin-walled cross-section types:
a – Type A; b – Type B, c – Type C

Accordingly, non-dimensional slenderness was equal to 1.082, 0.865, 0.650, 0.433 and 0.216. Notably, according to Eurocode 3-1-3 (CEN, 2006a), the width-to-thickness ratio of the web stiffener plate parts is constrained to 30 or less for S355 grade steel, rendering calculations beyond this threshold unfeasible. As a consequence of that, columns with stiffener width-to-thickness ratio greater than 30 were not calculated according to the Eurocode 3-1-3 (CEN, 2006a) design approach. The objective was to analyse the accuracy of the calculations across various width-to-thickness ratios of the stiffener, as this ratio is the key parameter when deciding the cross-section class of steel member parts. The thickness of the cross-section was attached to this ratio equal to 50, 40, 30, 20 and 10, rather than using a plain thickness value. Consequently, the thickness of the analysed cross-sections did not align with the production assortment.

Introducing Type C column cross-section allowed for further research of geometric possibilities utilizing the novel thin-walled column load-bearing resistance calculation method. This cross-section was based on the B cross section type, featured four bends in the web, representing four separate stiffeners. By analysing these diverse configurations, the objective was to assess the stiffener calculation and behaviour across various web stiffener designs within thin-walled columns.

The calculation results for Type A cross-section columns are presented in Figure 5, while those for Type B cross-section columns are provided in Figure 6. Definitions S1 and S3 respectively indicate the Eurocode 3-1-3 (CEN, 2006a) calculation algorithm for a single stiffener and the calculation algorithm proposed in this article with three stiffeners, followed by a number representing the length of the column in millimetres. The figures illustrate the percentage increase in the calculated load-bearing resistance of the columns when using the proposed method compared to design codes.

Load-bearing strength of columns with Type C cross-sections was exclusively calculated using the newly presented design methodology and is given in the numerical investigation section, where they are compared with finite element method analysis results.

The calculated slenderness of three separate stiffeners for Type A cross-section, as defined by the methodology described in this article, was lower than the slenderness calculated for a stiffener defined using the Eurocode 3-1-3 (CEN, 2006a) methodology. Consequently, this led to an increase in the effective cross-section area of the stiffeners and a subsequent increase of the column's load-bearing resistance. The load-bearing resistance calculated using this method ranged from 1.98% to 9.22% higher compared to that calculated according to the Eurocode 3-1-3 (CEN, 2006a) methodology. This difference grew when analysing shorter and thinner column cross-sections. However, the average load-bearing resistance calculated using the proposed method exhibited a 5.30% increase relative to the load-bearing strength computed in accordance with design codes for Type A column cross-sections. The calculation results of the load bearing strength for all column types are given in the Table 1.

Conversely, Type B column cross-section load-bearing calculation results exhibited minimal differences between the analysed methodologies, with a variation of up to 1.71%. Deeper stiffeners in column cross-sections proved to be more resistant to distortional buckling, resulting in a similar compound reduced effective cross-section area of the stiffeners when calculated according to both methodologies. This convergence explains the similarity in calculation results between the methodologies. The average load-bearing resistance, as determined by the proposed method, exhibited a slight increase of 0.37% compared to the load-bearing strength calculated according to design codes for Type B column cross-sections.

Overall, the proposed method was verified through a comparison of the calculated load-bearing strength of columns with various intermediate web stiffeners against both the proposed method and the design codes. The method exhibited greater consistency with design codes for columns with higher ratios of web height to stiffener depth.

5. Numerical investigation

Numerical models have been developed to verify the calculation results of the proposed method. Engineering simulation and 3D design software ANSYS (ANSYS, Inc., 2013) was selected for this purpose. The models incorporated both material and geometric non-linearity, alongside accounting for initial imperfections. Therefore, they fall under the classification of GMNIA models (Geometric and Material Non-linear Analysis with Imperfections).

Parametric analysis was conducted on column types A, B and C that are analysed in Section 4 (given in Figure 4). The numerical analysis compares the obtained results with the load-bearing strength calculated using both the newly proposed design approach and, where applicable, the conventional code-based methodology. This comparison provides insights into the effectiveness and applicability of the proposed approach in diverse scenarios.

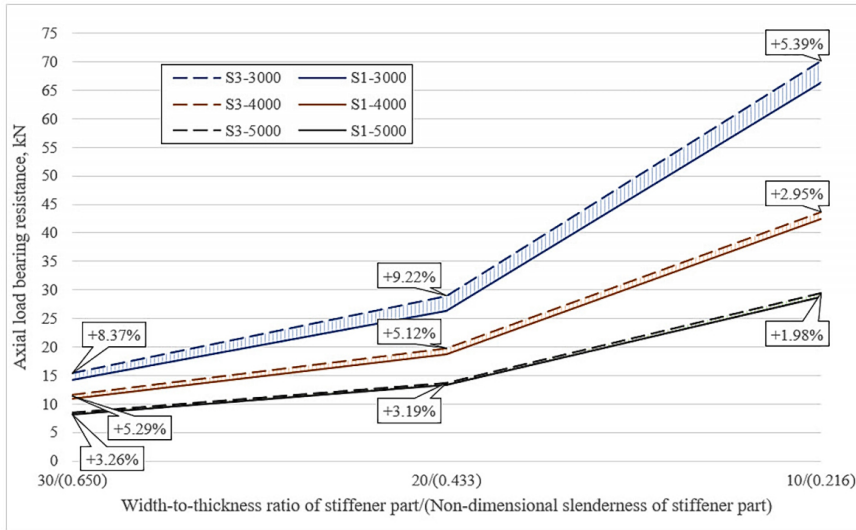


Figure 5. Column load bearing results with A Type column cross-section, S3 – proposed calculation method, S1 – single stiffener calculation method according to the Eurocode 3-1-3. Filled area between the lines represent the difference of the calculated load bearing strength between the calculation methods

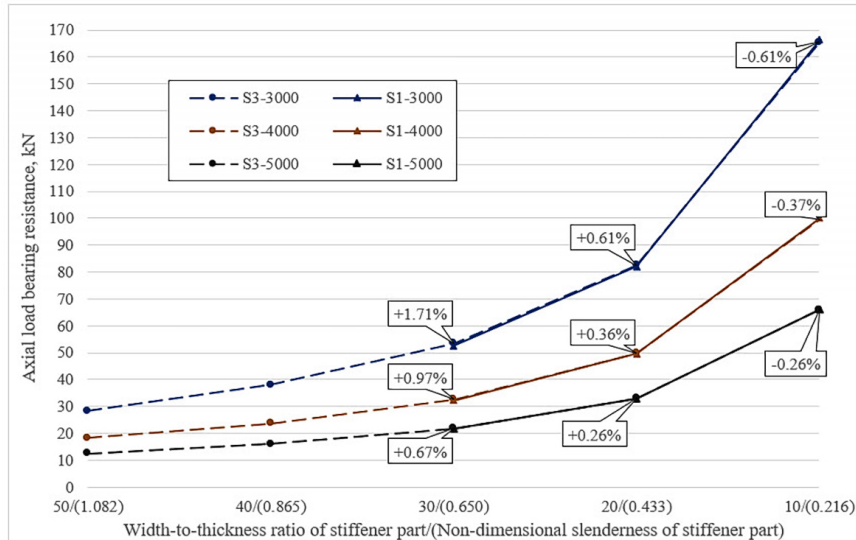


Figure 6. Calculated column load bearing results with B Type column cross-section, S3 – proposed calculation method, S1 – single stiffener calculation method according to the Eurocode 3-1-3

5.1. Material and geometrical properties

Bi-linear material non-linearity was included in the numerical model. The strain is calculated according to the Eurocode 3-1-14 draft (CEN, 2023) for cold-formed structures:

$$\epsilon = \begin{cases} \frac{\sigma}{E} + 0.002 \left(\frac{\sigma}{f_{yb}} \right)^8 & \text{for } \sigma \leq f_{yb} \\ \frac{\sigma - f_{yb}}{E_{0.2}} + \left(\epsilon_u - \epsilon_{0.2} - \frac{f_u - f_{yb}}{E_{0.2}} \right) \left(\frac{\sigma - f_{yb}}{f_u - f_{yb}} \right)^{1+3.3 \frac{f_{yb}}{f_u}} + \epsilon_{0.2} & \text{for } f_{yb} \leq \sigma \leq f_u \end{cases} \quad (10)$$

where ϵ is the strain, σ is the stress, E is the modulus of elasticity, f_{yb} is the basic yield stress, f_u is the ultimate strength. $E_{0.2}$ is the tangent modulus of the stress-strain curve at the yield strength calculated:

$$E_{0.2} = \frac{E}{1 + 0.016 \frac{E}{f_{yb}}} \quad (11)$$

The Young’s modulus and Poisson’s ratio values employed in finite element method analysis mirror those utilized in previous sections, set at 200 GPa and 0.3, respectively.

In this study, both column member and column cross-section imperfections were incorporated into the finite element model to enhance the accuracy of the analysis. These imperfections were applied to account for global, local, and distortional buckling modes, which are critical considerations in thin-walled column behaviour.

Imperfection sizes were selected according to the standard for steel structures execution (CEN, 2018). For

the global buckling mode, a column member imperfection was introduced using an $L/1000$ bar sinusoidal profile along the weak cross-section axis. This imperfection pattern mimicked the anticipated deviations from perfect straightness in the column member, which were characteristic to real-world structural elements subjected to compressive loading.

To simulate local and distortional buckling modes, imperfections were introduced by inducing buckling in the cross-section itself. The local and distortional imperfection to the cross-section plates were applied with a local and distortional buckling mode and an equivalent to $h/100$ for distortional buckling and $b_w/100$ for local buckling, where h and b_w represents the relevant width dimension of the cross-section, given in Figure 7. This imperfection captured the localized distortions and irregularities that could lead to local buckling, affecting the overall stability of the column.

Column load bearing strengths were calculated with global imperfection as well as local and distortional buckling mode imperfections applied to the cross-section. The imperfection type, causing the least load bearing resistance of the column was picked as the decisive imperfection. Imperfection modes applied to the analysed columns are given in Figure 7.

By implementing these imperfections, it was aimed to capture the realistic response of thin-walled columns, thereby improving the reliability of the finite element analysis and providing a detailed understanding of their structural behaviour.

In addition to geometric imperfections, cold-formed sections also exhibit residual stresses and material strengthening effects. Kishino et al. (2022) reported that residual stresses had only 2.8% impact, while residual strains had a negligible 1.0% effect on the buckling load of the cold-formed columns they examined. Furthermore, incorporating residual stresses into numerical analysis necessitates considering the effects of cold-working. Schafer et al. (2010) note that ignoring both effects under the as-

sumption of mutual offsetting is a common practice. Consequently, this research opted to exclude both from the simulation model.

5.2. Element type and finite element mesh

In the investigation, SHELL281 finite elements were employed in the models. SHELL281 finite elements are suitable for analysing thin to moderately thick shell structures. These elements have eight nodes with six degrees of freedom at each node. To ensure uniform stress distribution across the column cross-section, a thickness of 30 mm was designated for the column bases.

A mesh size of 15×15 mm was implemented for the column and its bases. This mesh resolution strikes a balance between computational efficiency and accuracy in capturing the structural response. Additionally, to enhance the precision of stiffener analysis, the finite element mesh was refined in proximity to the stiffener bends. This refinement targeted regions where significant stress concentrations and geometric complexities were anticipated, thereby optimizing the accuracy of the stiffener calculations. Illustrative representations of the typical finite element mesh employed for both the column and the base plate are provided in Figure 8.

5.3. Boundary conditions and loading procedure

The columns were analysed under a simply supported condition. Vertical, horizontal, and rotational supports were affixed to the mid-point of the base plate at the bottom of the column, while horizontal and rotational supports were secured to the top of the column's base plate.

To prevent collapse at the bottom support, the self-weight of the column was excluded from both the column and the base plates. Compressive deformation was applied to the midpoint of the top base plate to simulate external force. Acceptance criteria for the calculated Finite Element Method (FEM) results were a decreasing load-deformation

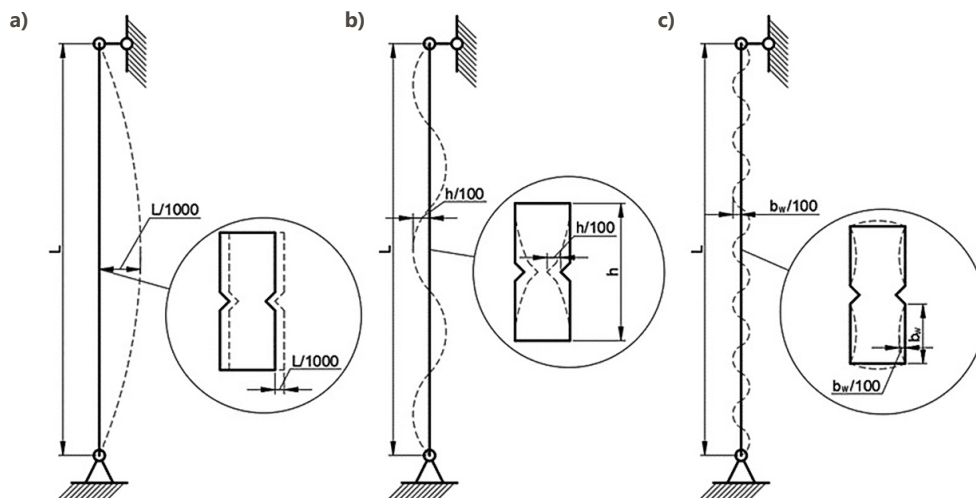


Figure 7. Imperfection modes for analysed columns: a – global imperfection; b – distortional imperfection; c – local imperfection

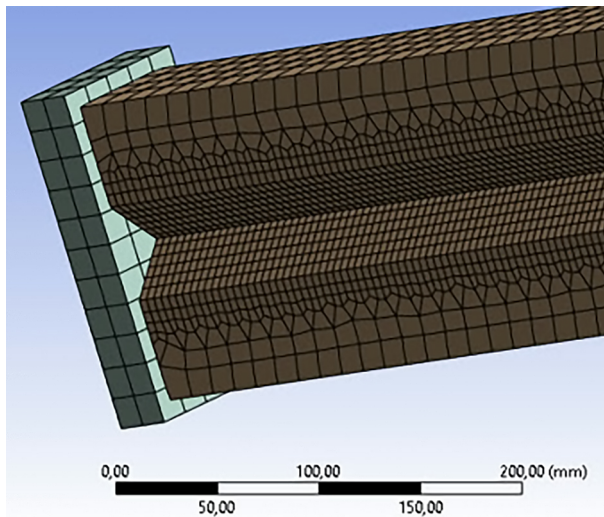


Figure 8. Element mesh of the column and the support base in the ANSYS software

ratio and attainment of the ultimate column strength within at least 25 load steps for each column. It was found that further increasing amount of load steps could influence not more than 0.5% of load bearing strength in this case as well as similar other case analysed by Schafer et al. (2010).

Acceptance criteria for the calculated Finite Element Method (FEM) results were a decreasing load-deformation ratio and attainment of the ultimate column strength within at least 25 load steps for each column.

5.4. Evaluation of calculated design strengths

The ANSYS analysis outcomes collectively reveal that among the various imperfections assessed, global imperfections emerged as the most critical across Type B and Type C columns, as well as a substantial portion of Type A columns. Specifically, Type A columns featuring a width-to-thickness ratio of the stiffener at 30 exhibited a deformed configuration characterized predominantly by local-global buckled deformation. Meanwhile, Type A columns spanning 3 meters and possessing a stiffener width-to-thickness ratio of 20 manifested a deformed state encompassing all buckling modes within the buckled deformation regime. Conversely, Type B and Type C columns exhibited resilience against local or distortional buckling phenomena owing to their comparatively greater thickness, ranging from 0.707 mm to 3.536 mm, coupled with an elevated column length. The principal deformed configurations of the buckled columns are visually shown in Figure 9.

For columns with Type A cross-sections and width-to-thickness ratios of 20 and 10, the load-bearing resistance was found to be more conservative when calculated according to Eurocode 3-1-3 (CEN, 2006a) design methodology, with results ranging from 17.82% to 6.51%. Conversely, calculation results using the methodology proposed in this article were less conservative, exhibiting deviations from

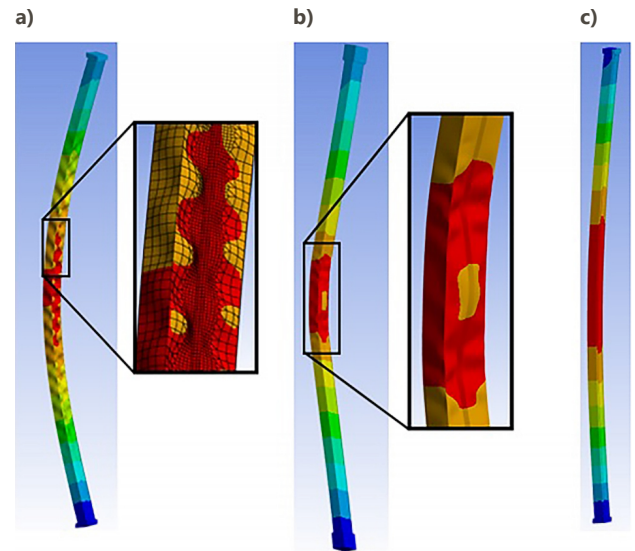


Figure 9. Deformed columns from the ANSYS calculations: a – local buckling with global buckling mode; b – interaction between local, distortional and global buckling modes, c – global buckling mode

9.47% to 4.22% compared to finite element analysis. The analysis results for these columns are detailed in Figure 10 and Table 1. Definitions S1, S3 and S4 respectively indicate the Eurocode 3-1-3 (CEN, 2006a) calculation algorithm for a single stiffener and the calculation algorithm proposed in this article with three and four stiffeners, followed by a number representing the length of the column in millimetres. The figures illustrate the percentage increase in the analytically calculated load-bearing resistance of the columns when compared to finite element method analysis.

The calculated load-bearing strength of columns, both in accordance with Eurocode 3-1-3 (CEN, 2006a) procedures and the proposed methodology, exhibited inaccuracies for Type A cross-sections with a stiffener width-to-thickness ratio of 30 in columns of 3 m and 4 m lengths. Upon analysing the column finite element model using ANSYS, it was observed that the load-bearing resistance remained consistent across various lengths due to the minimal local buckling strength of the cross-section. To analyse the case, an additional investigation was conducted utilizing open access finite strip analysis software, CUFSM (Li & Schafer, 2010; Schafer, 2020). The results revealed that the local buckling resistance of the cross-section was reached at 9.493 kN, maintaining this resistance throughout the column length range from 60 mm to 5000 mm. The critical elastic buckling load was computed by systematically varying the length of the column, under the assumption that the length corresponds to a single sine half-wave of transverse displacement. The resulting plot, known as the buckling signature curve of the column cross-section, illustrates this relationship. Figure 11a illustrates the signature curve along with the local buckling length and corresponding mode for the Type A cross-section, while Figure 11b illustrates the linear elastic critical buckling load

at different column lengths, with the buckling mode given at the 5000 mm column length. Notably, it was observed that the linear elastic buckling load and mode remained consistent between 60 mm and 5000 mm lengths, indicating that the column length had minimal impact on the load-bearing strength. Conversely, according to Eurocode 3-1-3 (CEN, 2006a), the length of the column significantly influences the calculation of the critical buckling load, a fundamental component in determining column slenderness (refer to Eqn (12) for the critical buckling load and

Eqn (13) for the column slenderness). Although the proportions of the cross-section geometry fell within the Eurocode 3-1-3 (CEN, 2006a) scope, requiring the width-to-thickness ratio of the flange and web to be less than 500 in closed cross-sections, in the analysed case, these ratios equated to 138 for the flange and 318 for the web. This case requires further attention and deeper analysis, though it lies beyond the scope of this article, and the results are not included in the subsequent analysis of the proposed calculation method validity.

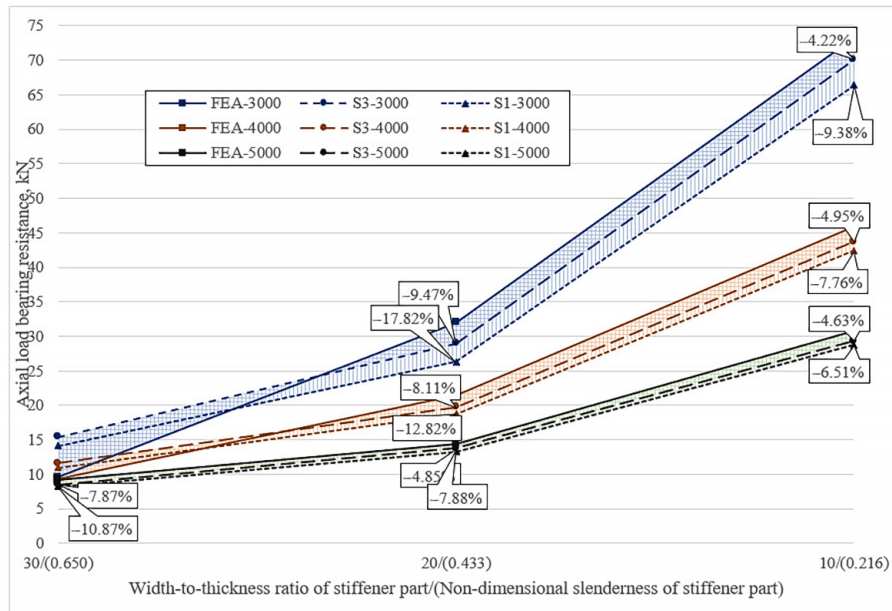


Figure 10. Load bearing resistance of column Type A cross-sections, S3 – proposed calculation method, S1 – single stiffener calculation method according to the Eurocode 3-1-3, AN – finite element analysis. Filled area between the lines represent the difference of the calculated load bearing strength between the calculation methods

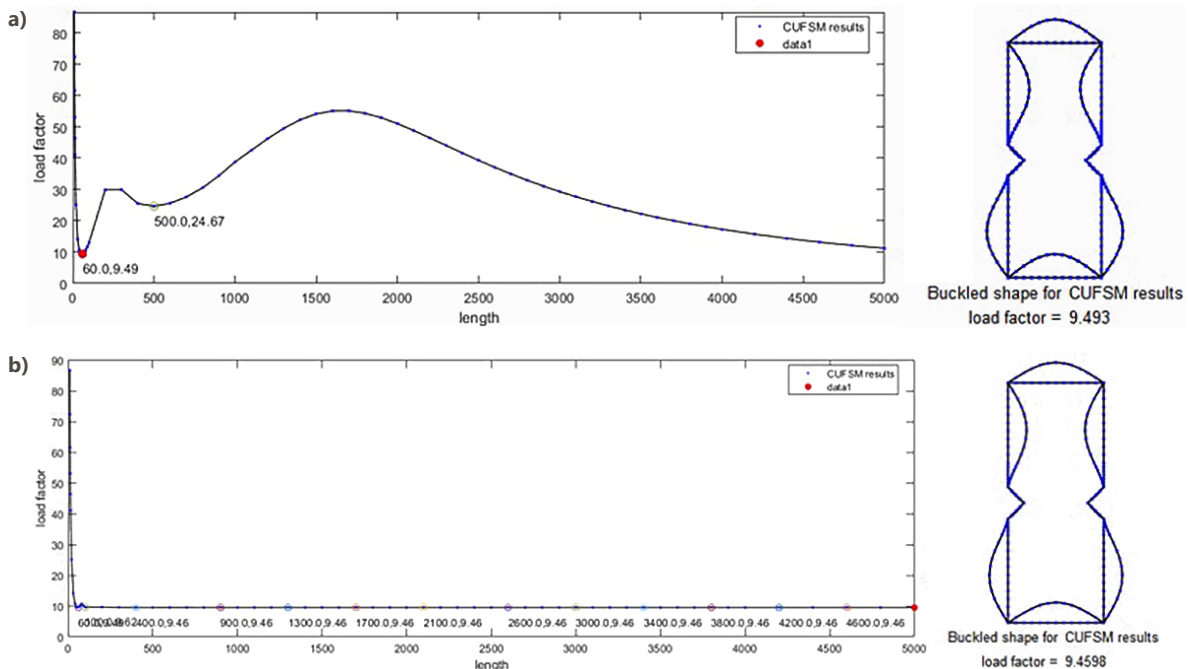


Figure 11. Linear buckling analysis results of a Type A cross-section of width-to-thickness ratio 30 using CUFM software: a – linear buckling load signature curve; b – linear buckling load of column at different column lengths

Critical buckling load of the column is calculated as follows:

$$N_{cr} = \frac{\pi^2 EI}{L^2}, \tag{12}$$

where E is the elasticity modulus, I is the second moment of cross-section area, L is the length of the column.

Slenderness of the column is calculated as follows:

$$\bar{\lambda} = \sqrt{\frac{A_{eff} f_{yb}}{N_{cr}}}, \tag{13}$$

where A_{eff} is the effective area of the cross-section, f_{yb} is the basic yield strength.

In contrast, Type B cross-section columns exhibited no errors in the calculated load-bearing strength results. Both calculation methods demonstrated good agreement with finite element method results across various column lengths and width-to-thickness ratios. Furthermore, extending the width-to-thickness area of analysis to ratios of 40 and 50 using the newly proposed calculation method yielded load-bearing strength trends closely aligned with finite element method design results. The calculated results were least conservative at the highest column lengths, with variations ranging from 2.63% to 5.68%, and most conservative at the lowest column lengths, ranging from 8.59% to 11.23%. The analysis results for these columns are detailed in Figure 12.

Across all combinations of column height and stiffener width-to-thickness ratios, the calculated load-bearing strength of columns with Type C cross-sections using the newly proposed calculation methodology proved accurate compared to finite element method analysis results. These calculated results exhibited a reserve of load-bearing strength ranging from 2.14% to 9.46%, with the reserve

increasing notably for shorter columns with thicker thicknesses. Detailed results for the calculated load-bearing strength of columns with Type C cross-sections are presented in Figure 13.

In summary, the load-bearing resistance, as determined by the proposed method, exhibited reductions of 6.29% for Type A, 6.71% for Type B, and 5.86% for Type C column cross-sections when compared to finite element method calculations. Collating across all column types, the mean reduction in load-bearing resistance amounted to 6.30%. The full results are given in Table 1.

In contrast, Dubina and Ungureanu (2023) provided a summary of load-bearing strength derived from numerical analysis and calculated based on Eurocode 3 standards. The results indicated that the calculated load-bearing strength of short columns according to Eurocode 3 was, on average, 8.4% smaller than the strength calculated numerically. The comparison between Dubina and Ungureanu (2023) and the result in this article is somewhat limited due to the analysis of non-identical scenarios. However, if compared, these results once again demonstrate that the newly proposed method yields slightly less conservative estimations of the load-bearing strength for columns with stiffeners.

The comprehensive findings derived from Finite Element Analysis reveal a consistent trend across all cases, wherein the load-bearing capacity of thin-walled columns exhibited an elevation when evaluated through finite element method-based software in contrast to the load-bearing strength computed using Eurocode methodology and the newly introduced procedure. Notably, the newly proposed procedure demonstrated load-bearing capacities that are comparatively less conservative when compared to the design codes.

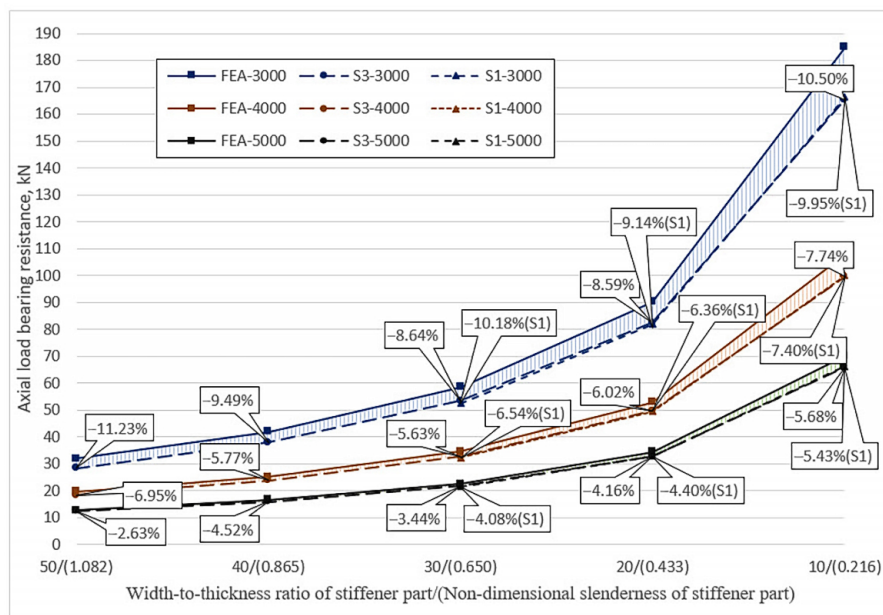


Figure 12. Load bearing resistance of column Type B cross-sections, S3 – proposed calculation method, S1 – single stiffener calculation method according to the Eurocode 3-1-3, FEA – finite element analysis. Filled area between the lines represent the difference of the calculated load bearing strength between the calculation methods

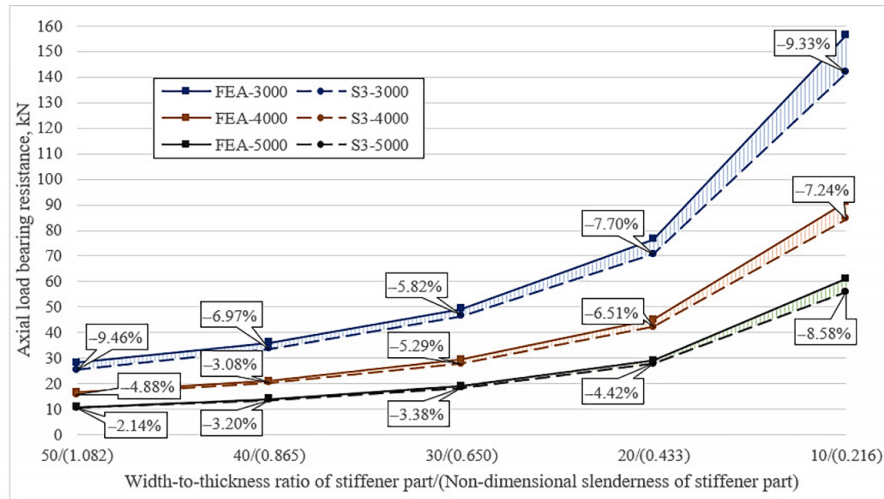


Figure 13. Load bearing resistance of column Type C cross-sections, S4 – proposed calculation method, FEA – finite element analysis. Filled area between the lines represent the difference of the calculated load bearing strength between the calculation methods

Table 1. Column load bearing results calculated according to the proposed method, Eurocode methodology and Finite Element Method

Cross-section type	Stiffener depth	Stiffener width-to-thickness ratio	Column length L , mm	Proposed method load bearing strength, kN	Eurocode method load bearing strength, kN	FEM load bearing strength, kN	Ratio of proposed to Eurocode method	Ratio of proposed method to FEM
Type A	$h/10$	10	3000	70.14	66.36	73.23	1.06	0.96
		10	4000	43.70	42.41	45.98	1.03	0.95
		10	5000	29.35	28.77	30.77	1.02	0.95
		20	3000	28.93	26.26	31.96	1.10	0.91
		20	4000	19.73	18.72	21.47	1.05	0.92
		20	5000	13.74	13.30	14.44	1.03	0.95
		30	3000	15.43	14.14	–	1.09	–
		30	4000	11.59	10.98	–	1.06	–
		30	5000	8.48	8.20	9.20	1.03	0.92
Average value for Type A							1.05	0.94
Type B	$h/6$	10	3000	165.40	166.42	184.80	0.99	0.90
		10	4000	99.64	100.01	108.00	1.00	0.92
		10	5000	66.02	66.20	70.00	1.00	0.94
		20	3000	82.45	81.96	90.20	1.01	0.91
		20	4000	49.73	49.56	52.92	1.00	0.94
		20	5000	32.97	32.89	34.40	1.00	0.96
		30	3000	53.43	52.53	58.48	1.02	0.91
		30	4000	32.61	32.30	34.56	1.01	0.94
		30	5000	21.73	21.58	22.50	1.01	0.97
		40	3000	38.01	–	42.00	–	0.91
		40	4000	23.75	–	25.20	–	0.94
		40	5000	15.97	–	16.72	–	0.96
		50	3000	28.41	–	32.00	–	0.89
		50	4000	18.31	–	19.68	–	0.93
50	5000	12.46	–	12.80	–	0.97		

End of Table 1

Cross-section type	Stiffener depth	Stiffener width-to-thickness ratio	Column length L , mm	Proposed method load bearing strength, kN	Eurocode method load bearing strength, kN	FEM load bearing strength, kN	Ratio of proposed to Eurocode method	Ratio of proposed method to FEM
Average value for Type B							1.00	0.93
Type C	$h/6$	10	3000	141.81	–	156.4	–	0.91
		10	4000	84.58	–	91.18	–	0.93
		10	5000	55.81	–	61.043	–	0.91
		20	3000	70.61	–	76.5	–	0.92
		20	4000	42.18	–	45.12	–	0.93
		20	5000	27.85	–	29.14	–	0.96
		30	3000	46.41	–	49.28	–	0.94
		30	4000	27.88	–	29.44	–	0.95
		30	5000	18.46	–	19.1	–	0.97
		40	3000	33.57	–	36.08	–	0.93
		40	4000	20.47	–	21.12	–	0.97
		40	5000	13.63	–	14.08	–	0.97
		50	3000	25.50	–	28.16	–	0.91
		50	4000	15.90	–	16.72	–	0.95
		50	5000	10.69	–	10.92	–	0.98
Average value for Type C							–	0.94
Average value for all types							1.03	0.94

6. Conclusions

In conclusion, this study introduced a novel approach for calculating intermediate web stiffeners in axially compressed thin-walled cross-section columns by treating each bend as an individual stiffener. This methodology enabled the design of cross-sections with three, four and potentially more intermediate web stiffeners, regardless of whether the plates between the web stiffener bends were under influence of the local buckling or not. Comparative analyses were conducted to assess the efficacy of the proposed method, wherein the load-bearing strength of columns was computed using both Eurocode 3-1-3 procedures and the newly proposed methodology. Various column types with ranges in length and thickness were analysed to verify the methodology.

The calculated load-bearing strength of Type A cross-section columns according to the newly proposed calculation methodology ranged from 1.98% to 9.22% higher compared to the Eurocode 3-1-3 (CEN, 2006a) procedures. Conversely, load-bearing strength calculations for Type B cross-section columns using both methodologies exhibited similarity, varying between –0.61% and 1.71%. Based on these findings, it can be concluded that column cross-sections featuring deeper stiffeners can be reliably analysed using the newly proposed calculation methodology. This conclusion is supported by the close alignment between the calculated load-bearing strength according

to this methodology and the design codes for such cross-sections.

Overall, the proposed approach for web stiffener calculation in thin-walled columns offers an effective means for cross-section design and provides valuable insights for engineers and researchers. The calculated load-bearing strength demonstrated less conservatism compared to Eurocode 3-1-3 (CEN, 2006a) methodology, with a reserve of 2.14% to 11.23% in analysed cases compared to finite element analysis results. These results verified the proposed method applicability for the analysis of thin-walled columns with intermediate web stiffeners.

The inception of the proposed method for analysing intermediate web stiffeners in thin-walled column cross-sections primarily aims at augmenting rather than altering the design approach outlined in the Eurocodes. Its principal objective lies in extending the applicability of design principles to cross-sectional configurations not accommodated by prevailing design codes, especially those featuring webs with stiffeners characterized by high slenderness ratios. Although the analytically calculated load-bearing strength of the columns could not be compared between the methods at high slenderness ratios of the stiffener, a comparison of the proposed method results with the finite element analysis method results demonstrated great consistency and accurately estimated analytical load-bearing strength capacity in such cases. These results verified that the geometric limitations can be expanded when employ-

ing the proposed method, in comparison to the design codes. Thin-walled cross-sections with stiffeners featuring width-to-thickness ratios up to 30 undergo analysis using the design approach outlined in Eurocode 3. However, for cross-sections characterized by higher stiffener width-to-thickness ratios, ranging from 30 to 50 and beyond, the methodology presented in this article is recommended for application.

Furthermore, it is anticipated that this approach could be readily adapted for application to thin-walled members subjected to combined loading scenarios involving bending and compression. Future investigations could focus on studying the behaviour of web stiffeners under combined axial and bending loads or exploring other cross-section types and design parameters, including different stiffener amount, to enhance our understanding of their influence on structural performance.

Acknowledgements

The authors would like to express their gratitude to the editor and the anonymous reviewers for handling and reviewing the paper.

Funding

The research didn't have any external funding.

Author contributions

Mantas Stulpinas, under supervision of Alfonsas Daniūnas, compiled the methodology, performed analysis, investigation, and writing.

Disclosure statement

The authors declare that they do not have any competing financial, professional, or personal interests from other parties.

References

- Abdoh, D. A. (2024). Three-dimensional peridynamic modeling of deformations and fractures in steel beam-column welded connections. *Engineering Failure Analysis*, 160, Article 108155. <https://doi.org/10.1016/j.engfailanal.2024.108155>
- Alabi-Bello, M., A., Wang, Y., C., & Su, M. (2021). An assessment of different direct strength methods for cold-formed thin-walled steel beam-columns under compression and major axis bending. *Structures*, 34, 4788–4802. <https://doi.org/10.1016/j.istruc.2021.10.027>
- ANSYS, Inc. (2013). *ANSYS mechanical APDL verification manual*.
- Ananthi, G. B. G., Deepak, M. S., Roy, K., & Lim, J. B. P. (2021). Influence of intermediate stiffeners on the axial capacity of cold-formed steel back-to-back built-up unequal angle sections. *Structures*, 32, 827–848. <https://doi.org/10.1016/j.istruc.2021.03.059>
- Bučmys, Ž., Daniūnas, A., Jaspert, J.-P., & Demonceau, J.-F. (2018). A component method for cold-formed steel beam-to-column bolted gusset plate joints. *Thin-Walled Structures*, 123, 520–527. <https://doi.org/10.1016/j.tws.2016.10.022>
- Chen, J., He, Y., Jin, W. L. (2010). Stub column tests of thin-walled complex section with intermediate stiffeners. *Thin-Walled Structures*, 48(6), 423–429. <https://doi.org/10.1016/j.tws.2010.01.008>
- Cheng, L., Qiu, C., & Du, X. (2024). A two-level performance-based plastic design method for multi-story steel frames with double-yielding systems. *Soil Dynamics and Earthquake Engineering*, 178, Article 108449. <https://doi.org/10.1016/j.soildyn.2024.108449>
- Dar, M., A., Verma, A., Anbarasu, M., Pang, S., D., & Dar, A. R. (2022). Design of cold-formed steel battened built-up columns. *Journal of Constructional Steel Research*, 193, Article 107291. <https://doi.org/10.1016/j.jcsr.2022.107291>
- Dong, S., Li, H., & Wen, Q. (2015). Study on distortional buckling performance of cold-formed thin-walled steel flexural members with stiffeners in the flange. *Thin-Walled Structures*, 95, 161–169. <https://doi.org/10.1016/j.tws.2015.07.006>
- Dubina, D., & Ungureanu, V. (2023). Local/distortional and overall interactive buckling of thin-walled cold-formed steel columns with open cross-section. *Thin-Walled Structures*, 182, Article 110172. <https://doi.org/10.1016/j.tws.2022.110172>
- European Committee for Standardization. (2006a). *Eurocode 3: Design of steel structures – Part 1-3: General rules – Supplementary rules for cold-formed members and sheeting* (EN 1993-1-3).
- European Committee for Standardization. (2006b). *Eurocode 3: Design of steel structures – Part 1-5: Plated structural elements* (EN 1993-1-5).
- European Committee for Standardization. (2018). *Execution of steel structures and aluminium structures – Part 2: Technical requirements for steel structures* (EN 1090-2:2018).
- European Committee for Standardization. (2023). *Eurocode 3: Design of steel structures – Part 1-14: Design assisted by finite element analysis* (EN 1993-1-14).
- Gurupatham, B. G. A., Roy, K., Raftery, G. M., & Lim, J. B. P. (2022). Influence of intermediate stiffeners on axial capacity of thin-walled built-up open and closed channel section columns. *Buildings*, 12(8), Article 1071. <https://doi.org/10.3390/buildings12081071>
- Habashneh, M., Cucuzza, R., Domaneschi, M., & Movahedi Rad, M. (2024). Advanced elasto-plastic topology optimization of steel beams under elevated temperatures. *Advances in Engineering Software*, 190, Article 103596. <https://doi.org/10.1016/j.advensoft.2024.103596>
- Kherbouche, S., & Megnounif, A. (2019). Numerical study and design of thin walled cold formed steel built-up open and closed section columns. *Engineering Structures*, 179, 670–682. <https://doi.org/10.1016/j.engstruct.2018.10.069>
- Kishino, V. H., Kishino, R. T., & Coda, H. B. (2022). A sequential investigation of the residual stresses and strains influence on the buckling of cold-formed thin-walled members. *Thin-Walled Structures*, 180, Article 109814. <https://doi.org/10.1016/j.tws.2022.109814>
- Kotelko, M. (2007). Load-carrying capacity and energy absorption of thin-walled profiles with edge stiffeners. *Thin-Walled Structures*, 45(10–11), 872–876. <https://doi.org/10.1016/j.tws.2007.08.038>
- Laghi, V., Babovic, N., Benvenuti, E., & Kloft, H. (2024). Blended structural optimization of steel joints for wire-and-arc additive manufacturing. *Engineering Structures*, 300, Article 117141. <https://doi.org/10.1016/j.engstruct.2023.117141>
- Li, Z., & Schafer, B. W. (2010). Buckling analysis of cold-formed steel members with general boundary conditions using CUFSM

- conventional and constrained finite strip methods. In *CCFSS Proceedings of International Specialty Conference on Cold-Formed Steel Structures* (pp. 1971–2018). Missouri University of Science and Technology. <https://scholarsmine.mst.edu/isccss/20iccfss/20iccfss-session1/2>
- Li, Q. Y., & Young, B. (2023). Experimental and numerical studies on cold-formed steel battened columns. *Engineering Structures*, 288, Article 116110. <https://doi.org/10.1016/j.engstruct.2023.116110>
- Li, Q. Y., & Young, B. (2024). Experimental and numerical investigation on cold-formed steel zed section beams with complex edge stiffeners. *Thin-Walled Structures*, 194, Article 111315. <https://doi.org/10.1016/j.tws.2023.111315>
- Liu, C., Chen, X., Mao, X., He, L., & Yuan, J. (2023). Study on flexural and demountable behavior of a modular light-gauge steel framed wall. *Journal of Civil Engineering and Management*, 29(2), 143–156. <https://doi.org/10.3846/jcem.2023.18351>
- Meza, F., J., & Becque, J. (2023). Numerical modelling of cold-formed steel built-up columns. *Thin-Walled Structures*, 188, Article 110781. <https://doi.org/10.1016/j.tws.2023.110781>
- Meza, F., J., Becque, J., & Hajirasouliha, I. (2020). Experimental study of the cross-sectional capacity of cold-formed steel built-up columns. *Thin-Walled Structures*, 155, Article 106958. <https://doi.org/10.1016/j.tws.2020.106958>
- Mojtabaei, S., M., Hajirasouliha, I., & Ye, J. (2021). Optimisation of cold-formed steel beams for best seismic performance in bolted moment connections. *Journal of Constructional Steel Research*, 181, Article 106621. <https://doi.org/10.1016/j.jcsr.2021.106621>
- Mokhtari, F., & Imanpour, A. (2024). Hybrid data-driven and physics-based simulation technique for seismic analysis of steel structural systems. *Computers & Structures*, 295, Article 107286. <https://doi.org/10.1016/j.compstruc.2024.107286>
- Natali, A., & Morelli, F. (2022). Experimental validation of dissipative reduced-section thin walled diagonals for seismic-resistant automated rack supported warehouses. *Procedia Structural Integrity*, 44, 2334–2341. <https://doi.org/10.1016/j.prostr.2023.01.298>
- Rinchen, R., & Rasmussen, K. J. R. (2020). Experiments on long-span cold-formed steel single C-section portal frames. *Journal of Structural Engineering*, 146(1), Article 04019187. [https://doi.org/10.1061/\(ASCE\)ST.1943-541X.0002487](https://doi.org/10.1061/(ASCE)ST.1943-541X.0002487)
- Sang, L., Zhou, T., Zhang, L., Chen, B., & Wang, S. (2022). Experimental investigation on the axial compression behavior of cold-formed steel triple-limbs built-up columns with half open section. *Thin-Walled Structures*, 172, Article 108913. <https://doi.org/10.1016/j.tws.2022.108913>
- Schafer, B. W. (2011). Cold-formed steel structures around the world. *Steel Construction*, 4(3), 141–149. <https://doi.org/10.1002/stco.201110019>
- Schafer, B., W. (2020, April 6). Intro to CUFSM. *CUFSM – Cross-section elastic buckling analysis. Constrained and unconstrained finite strip method*. <https://www.ce.jhu.edu/cufsm/2020/04/06/intro-to-cufsm/>
- Schafer, B. W., Li, Z., & Moen, C. D. (2010). Computational modeling of cold-formed steel. *Thin-Walled Structures*, 48(10–11), 752–762. <https://doi.org/10.1016/j.tws.2010.04.008>
- Seyedabadi, M. R., Karrabi, M., Shariati, M., Karimi, S., Maghreb, M., & Eicker, U. (2024). Global building life cycle assessment: Comparative study of steel and concrete frames across European Union, USA, Canada, and Australia building codes. *Energy and Buildings*, 304, Article 113875. <https://doi.org/10.1016/j.enbuild.2023.113875>
- Stulpinas, M., & Daniūnas, A. (2024). Selection of an optimum axially compressed closed cross-section thin-walled built-up column. In J. A. O. Barros, G. Kaklauskas, & E. K. Zavadskas (Eds.), *Lecture notes in civil engineering, Vol. 392: Modern building materials, structures and techniques (MBMST 2023)* (pp. 194–203). Springer, Cham. https://doi.org/10.1007/978-3-031-44603-0_19
- Truong, D. N., & Chou, J. S. (2023). Integrating enhanced optimization with finite element analysis for designing steel structure weight under multiple constraints. *Journal of Civil Engineering and Management*, 29(8), 757–786. <https://doi.org/10.3846/jcem.2023.20399>
- Weixin, M., Jurgen, B., Iman, H., & Jun, Y. (2015). Cross-sectional optimization of cold-formed steel channels to Eurocode 3. *Engineering Structures*, 101, 641–651. <https://doi.org/10.1016/j.engstruct.2015.07.051>
- Wen, C.-B., Zhu, B.-L., Sun, H.-J., Guo, Y.-L., Zheng, W.-J., & Deng, L.-L. (2024). Global stability design of double corrugated steel plate shear walls under combined shear and compression loads. *Thin-Walled Structures*, 199, Article 111789. <https://doi.org/10.1016/j.tws.2024.111789>
- Ye, J., Quan, G., Kyvelou, P., Teh, L., & Gardner, L. (2022). A practical numerical model for thin-walled steel connections and built-up members. *Structures*, 38, 753–764. <https://doi.org/10.1016/j.istruc.2022.02.028>
- Zhang, X., & Rasmussen, K. (2014). Tests of cold-formed steel portal frames with slender sections. *Steel Construction*, 7, 199–203. <https://doi.org/10.1002/stco.201410030>
- Zhang, J., H., & Young, B. (2018a). Experimental investigation of cold-formed steel built-up closed section columns with web stiffeners. *Journal of Constructional Steel Research*, 147, 380–392. <https://doi.org/10.1016/j.jcsr.2018.04.008>
- Zhang, J., H., & Young, B. (2018b). Finite element analysis and design of cold-formed steel built-up closed section columns with web stiffeners. *Thin-Walled Structures*, 131, 223–237. <https://doi.org/10.1016/j.tws.2018.06.008>
- Zhou, K., Li, Q. S., Zhi, L. H., Han, X. L., & Xu, K. (2023). Investigation of modal parameters of a 600-m-tall skyscraper based on two-year-long structural health monitoring data and five typhoons measurements. *Engineering Structures*, 274, Article 115162. <https://doi.org/10.1016/j.engstruct.2022.115162>